Measurement of the Λ_c^+ lifetime

F. Abudinén, L. Aggarwal, H. Ahmed, J. K. Ahn, H. Aihara, N. Akopov, A. Aloisio, N. Anh Ky, D. M. Asner, H. Atmacan, T. Aushev, V. Aushev, V. Babu, H. Bae, P. Bambade, Sw. Banerjee, S. Bansal, J. Baudot, M. Bauer, A. Baur, A. Beaubien, J. Becker, J. V. Bennett, E. Bernieri, F. U. Bernlochner, V. Bertacchi, M. Bertemes, E. Bertholet, M. Bessner, S. Bettarini, V. Bhardwaj, F. Bianchi, T. Bilka, D. Biswas, D. Bodrov, A. Bolz, G. Bonvicini, A. Bozek, M. Bračko, P. Branchini, R. A. Briere, T. E. Browder, A. Budano, S. Bussino, M. Campajola, L. Cao, G. Casarosa, C. Cecchi, M.-C. Chang, P. Chang, R. Cheaib, P. Cheema, C. Chen, Y. Q. Chen, Y.-T. Chen, B. G. Cheon, K. Chilikin, K. Chirapatpimol, H.-E. Cho, K. Cho, S.-J. Cho, S.-K. Choi, S. Choudhury, D. Cinabro, L. Corona, L. M. Cremaldi, S. Cunliffe, F. Dattola, E. De La Cruz-Burelo, S. A. De La Motte, G. De Nardo, M. De Nuccio, G. De Pietro, R. de Sangro, M. Destefanis, A. De Yta-Hernandez, R. Dhamija, A. Di Canto, F. Di Capua, J. Dingfelder, Z. Doležal, I. Domínguez Jiménez, T. V. Dong, M. Dorigo, K. Dort, D. Dossett, S. Dreyer, G. Dujany, M. Eliachevitch, D. Epifanov, P. Feichtinger, T. Ferber, D. Ferlewicz, T. Fillinger, G. Finocchiaro, K. Flood, A. Fodor, F. Forti, A. Frey, B. G. Fulsom, A. Gabrielli, E. Ganiev, M. Garcia-Hernandez, A. Gaz, A. Gellrich, G. Ghevondyan, R. Giordano, A. Giri, A. Glazov, B. Gobbo, R. Godang, P. Goldenzweig, W. Gradl, S. Granderath, D. Greenwald, T. Gu, Y. Guan, K. Gudkova, J. Guilliams, S. Halder, K. Hara, O. Hartbrich, K. Hayasaka, H. Hayashii, S. Hazra, C. Hearty, I. Heredia de la Cruz, M. Hernández Villanueva, A. Hershenhorn, T. Higuchi, M. Hohmann, T. Humair, T. Iijima, K. Inami, G. Inguglia, N. Ipsita, A. Ishikawa, S. Ito, R. Itoh, M. Iwasaki, Y. Iwasaki, P. Jackson, W. W. Jacobs, D. E. Jaffe, Q. P. Ji, Y. Jin, H. Junkerkalefeld, M. Kaleta, J. Kandra, K. H. Kang, R. Karl, G. Karyan, C. Kiesling, C.-H. Kim, D. Y. Kim, K.-H. Kim, Y.-K. Kim, H. Kindo, K. Kinoshita, P. Kodyš, T. Koga, S. Kohani, K. Kojima, A. Korobov, S. Korpar, E. Kovalenko, R. Kowalewski, T. M. G. Kraetzschmar, P. Križan, P. Krokovny, T. Kuhr, J. Kumar, R. Kumar, K. Kumara, T. Kunigo, Y.-J. Kwon, S. Lacaprara, T. Lam, L. Lanceri, J. S. Lange, M. Laurenza, R. Leboucher, S. C. Lee, P. Leitl, D. Levit, L. K. Li, S. X. Li, Y. B. Li, J. Libby, Z. Liptak, Q. Y. Liu, D. Liventsev, S. Longo, T. Lueck, C. Lyu, M. Maggiora, R. Maiti, S. Maity, R. Manfredi, E. Manoni, S. Marcello, C. Marinas, L. Martel, A. Martini, L. Massaccesi, M. Masuda, K. Matsuoka, D. Matvienko, J. A. McKenna, F. Meier, M. Merola, M. Milesi, C. Miller, K. Miyabayashi, G. B. Mohanty, N. Molina-Gonzalez, S. Moneta, H. Moon, H.-G. Moser, M. Mrvar, R. Mussa, I. Nakamura, M. Nakao, H. Nakayama, A. Narimani Charan, M. Naruki, Z. Natkaniec, A. Natochii, L. Nayak, M. Nayak, G. Nazaryan, C. Niebuhr, N. K. Nisar, S. Nishida, K. Nishimura, H. Ono, P. Oskin, E. R. Oxford, G. Pakhlova, A. Paladino, A. Panta, E. Paoloni, S. Pardi, K. Parham, H. Park, S.-H. Park, A. Passeri, T. K. Pedlar, I. Peruzzi, R. Peschke, R. Pestotnik, F. Pham, L. E. Piilonen, G. Pinna Angioni, P. L. M. Podesta-Lerma, T. Podobnik, S. Pokharel, L. Polat, C. Praz, S. Prell, E. Prencipe, M. T. Prim, H. Purwar, N. Rad, P. Rados, S. Raiz, M. Reif, S. Reiter, I. Ripp-Baudot, G. Rizzo, S. H. Robertson, J. M. Roney, A. Rostomyan, N. Rout, G. Russo, D. A. Sanders, S. Sandilya, A. Sangal, L. Santelj, Y. Sato, V. Savinov, B. Scavino, C. Schwanda, A. J. Schwartz, Y. Seino, A. Selce, K. Senyo, J. Serrano, C. Sfienti, C. P. Shen, T. Shillington, J.-G. Shiu, A. Sibidanov, F. Simon, R. J. Sobie, A. Soffer, A. Sokolov, E. Solovieva, S. Spataro, B. Spruck, M. Starič, S. Stefkova, R. Stroili, J. Strube, M. Sumihama, K. Sumisawa, W. Sutcliffe, S. Y. Suzuki, H. Svidras, M. Takahashi, M. Takizawa, U. Tamponi, S. Tanaka, K. Tanida, H. Tanigawa, N. Taniguchi, F. Tenchini, R. Tiwary, D. Tonelli, E. Torassa, N. Toutounji, K. Trabelsi, M. Uchida, K. Unger, Y. Unno, K. Uno, S. Uno, P. Urquijo, Y. Ushiroda, S. E. Vahsen, R. van Tonder, G. S. Varner, K. E. Varvell, A. Vinokurova, L. Vitale, V. Vobbilisetti, E. Waheed, H. M. Wakeling, E. Wang, M.-Z. Wang, X. L. Wang, A. Warburton, S. Watanuki, M. Welsch, C. Wessel, J. Wiechczynski, H. Windel, E. Won, X. P. Xu, B. D. Yabsley, S. Yamada, S. B. Yang, H. Ye, J. Yelton, J. H. Yin, K. Yoshihara, Y. Yusa, Y. Zhang, V. Zhilich, Q. D. Zhou, V. I. Zhukova, and R. Žlebčík

(The Belle II Collaboration)

An absolute measurement of the Λ_c^+ lifetime is reported using $\Lambda_c^+ \to pK^-\pi^+$ decays in events reconstructed from data collected by the Belle II experiment at the SuperKEKB asymmetric-energy electron-positron collider. The total integrated luminosity of the data sample, which was collected at center-of-mass energies at or near the $\Upsilon(4S)$ resonance, is $207.2\,\text{fb}^{-1}$. The result, $\tau(\Lambda_c^+) = 203.20 \pm 0.89\,(\text{stat}) \pm 0.77\,(\text{syst})\,\text{fs}$, is the most precise measurement to date and is consistent with previous determinations.

Searches for physics beyond the standard model of particle physics through precise measurements of weakly decaying charm or bottom hadrons often rely on accurate theoretical descriptions of strong interactions at low energy, typically using effective models such as the heavy quark expansion (HQE) [1–7]. The HQE provides a consistent framework for computing the decay widths of heavy hadrons in terms of inverse powers of the heavy quark mass. For bottom hadrons, non-perturbative effects are relatively small and the HQE in $1/m_b$, where m_b is the mass of the bottom quark, works well. In contrast, higher-order corrections due to the influence of light valence (spectator) quarks are significant for charm hadron lifetimes, for which the HQE to $1/m_c^3$ does not satisfactorily describe lifetimes [7]. The lifetimes of the Ω_c^0 and Ξ_c^0 were recently measured to be much larger than the previous world average [8–10], inverting the known hierarchy of charm lifetimes. Careful consideration of model-dependent spectator effects is required for theoretical predictions of charm baryon lifetimes to agree with experimental measurements [6, 7]. Improved measurements of charm baryon lifetimes therefore provide refined tests for effective models.

The world average value of the Λ_c^+ lifetime is $202.4 \pm 3.1\,\text{fs}$ [11]. Previous measurements include percent-level results from the FOCUS, SELEX, and CLEO collaborations two decades ago [12–14], as well as a more precise measurement, relative to the D^+ lifetime, from the LHCb collaboration [9]. The latter of these has a limiting systematic uncertainty associated with the D^+ lifetime. Relative measurements minimize systematic uncertainties related to event selection that may bias the decay time, particularly at hadron colliders. In contrast, the ability to reconstruct charm hadrons without biasing the decay time allows experiments at electron-positron (e^+e^-) colliders to precisely determine absolute lifetimes, as demonstrated by the recent measurement of the D^0 and D^+ lifetimes [15] from the Belle II experiment [16] at the SuperKEKB asymmetric-energy e^+e^- collider [17]. The most recent Λ_c^+ lifetime measurement at an e^+e^- collider, from the CLEO collaboration, is in mild tension with other results and increases the uncertainty of the world average [11]. A precise, absolute measurement by Belle II may help to resolve the tension between Λ_c^+ lifetime measurements at e^+e^- colliders and other experiments and will substantially improve the world average.

In this Letter, we report a precise measurement of the Λ_c^+ lifetime using $\Lambda_c^+ \to pK^-\pi^+$ decays reconstructed in data collected at or near the $\Upsilon(4S)$ resonance, corre-sponding to a center of mass energy at or near $10.58\,\text{GeV}$, by the Belle II experiment from 2019 to mid 2021 and corresponding to an integrated luminosity of $207.2\,\text{fb}^{-1}$. Unless specified otherwise, charge conjugate decays are implied throughout.

The lifetime of the Λ_c^+ is determined from a two-dimensional fit to the decay time t and its uncertainty σ_t. The decay time is calculated assuming that Λ_c^+ candidates are promptly produced from continuum $e^+e^- \to c\bar{c}$ events and is determined according to $t = m_{\Lambda_c} \vec{L} \cdot \vec{p}/|\vec{p}|^2$, where m_{Λ_c} is the world average mass of the Λ_c^+ [11], $\vec{L}$ is the displacement of the Λ_c^+ decay point from the e^+e^- interaction point (IP), and $\vec{p}$ is the momentum of the Λ_c^+ candidate. The position and size of the IP region is determined using $e^+e^- \to \mu^+\mu^-$ events. Event selection criteria and the fit strategy are optimized and validated using simulated data, but the fit to the collision data does not use any input taken from simulation.

The Belle II detector [16] includes a tracking system comprising a two-layer silicon pixel detector (PXD) surrounded by a four-layer double-sided silicon strip detector (SVD) and a 56-layer central drift chamber (CDC). The second layer of the PXD had 15% azimuthal coverage during the collection of the data used in this study. For the Λ_c^+ decays considered here, the combined PXD and SVD vertexing system provide a decay-length resolution of $40\,\mu\text{m}$, corresponding to an average decay time resolution of $87\,\text{fs}$ for an average decay length of $96\,\mu\text{m}$. A time-of-propagation counter in the barrel region of the detector and an aerogel ring-imaging Cherenkov counter in the endcap region provide charged-particle identification (PID) information. An electromagnetic calorimeter consisting of CsI(Tl) crystals provides energy and timing measurements for photons and electrons. A K_L^0 and muon detector is installed in the iron flux return yoke of a superconducting solenoid magnet that provides a $1.5\,\text{T}$ magnetic field.

We generate $e^+e^- \to q\bar{q}$ events with KKMC [18] and hadronize quarks with Pythia 8 [19]. Hadron decays are emulated using EvtGen [20]. The detector response is simulated with Geant4 [21]. Reconstruction of events from simulated and collision data is performed with the Belle II analysis software framework [22]. In addition to the excellent vertexing capability, Belle II benefits from good charged particle tracking performance [23, 24].

Candidate $\Lambda_c^+ \to pK^-\pi^+$ decays are each reconstructed from one negatively and two positively charged particles, which are required to be well measured with reliable uncertainties to allow for a precise lifetime mea-

surement. Each charged particle must be associated with one or more PXD measurements (hits) in the PXD, at least one hit in the first layer of the SVD, and at least 20 hits in the CDC. Each charged particle must have a distance of closest approach to the IP of less than 0.5 cm in the plane transverse to the beam and 2 cm in the direction parallel to it to remove charged particles not associated with the e^+e^- interaction. A fit constrains the charged particles to come from a common vertex and the Λ_c^+ candidate to come from the IP [25]. Candidates with a vertex-fit χ^2 probability less than 0.01 are rejected. Since the Λ_c^+ is assumed to originate from the IP, secondary decays in which the Λ_c^+ originates from a displaced vertex would bias the lifetime measurement. To suppress Λ_c^+ from B decays, the center-of-mass momentum of each Λ_c^+ candidate is required to be greater than 2.5 GeV/c.

Charged PID information is combined from all subdetector systems except the PXD and SVD. This PID information is used to construct likelihoods $\mathscr{L}(h)$ for a given particle hypothesis h. For each candidate, one positively charged particle is required to have $\mathscr{L}(p)/(\mathscr{L}(p) + \mathscr{L}(K) + \mathscr{L}(\pi)) > 0.9$, the negatively charged particle is required to have $\mathscr{L}(K)/(\mathscr{L}(p) + \mathscr{L}(K) + \mathscr{L}(\pi) + \mathscr{L}(\mu) + \mathscr{L}(e) + \mathscr{L}(d)) > 0.6$, and the remaining positively charged particle is assumed to be a pion. Here $\mathscr{L}(d)$ is the deuteron hypothesis likelihood. The efficiency of the proton identification is found to be about 88%, with a kaon contamination of less than 2%, and the efficiency of kaon identification is 70%, with a pion contamination of 6%, from studies of $\Lambda^0 \to p\pi^-$ and D^{*+}-tagged $D^0 \to K^-\pi^+$ decays. To reduce backgrounds from misidentified charm-meson decays, we reject events with $M(\pi^+K^-\pi^+)$ in [1.858, 1.881] GeV/c^2 or [2.000, 2.020] GeV/c^2, with both positively charged particles assumed to be pions. These intervals correspond to three units of resolution, or standard deviations, on the reconstructed mass in both directions around the known D^+ and D^{*+} masses, respectively. Other charm-related backgrounds are suppressed by requiring that the transverse momenta of pions exceed 0.35 GeV/c and those of protons exceed 0.7 GeV/c.

Events with multiple candidates, which occur at a rate of 0.2%, are rejected. Analysis of simulated events shows that the event selection criteria do not bias the measurement of the Λ_c^+ lifetime.

Decays of $\Xi_c^0 \to \pi^-\Lambda_c^+$ and $\Xi_c^+ \to \pi^0\Lambda_c^+$ may bias the measurement of the Λ_c^+ lifetime, since the Ξ_c^0 and Ξ_c^+ have lifetimes of 153 ± 6 fs and 456 ± 5 fs [11], respectively, and may shift the production vertex of the Λ_c^+ away from the IP. The amount of Ξ_c contamination is estimated from a fit to the distribution of the Λ_c^+ vertex displacement from the IP in the plane transverse to the beam line. This distribution depends only on the resolution of the detector for Λ_c^+ candidates that are produced at the IP. Λ_c^+ candidates from Ξ_c decays

have production vertices that are displaced from the IP and therefore a larger vertex displacement from the IP. The fit to the distribution of the Λ_c^+ transverse vertex displacement gives a background contamination of 374 $\pm$ 88 events, corresponding to 0.003% of Λ_c^+ candidates. As this includes both combinatoric backgrounds and Ξ_c decays, the central value is taken as an estimate of the maximum number of Ξ_c decays. This value is consistent with predictions based on the expected production cross-sections for Ξ_c^0 and Ξ_c^+ [26], the measured branching fraction for $\Xi_c^0 \to \pi^-\Lambda_c^+$ [27], and theoretical predictions for $\Xi_c^+ \to \pi^0\Lambda_c^+$ [28]. Backgrounds from Ξ_c decays are reduced by restricting the invariant mass of the Ξ_c candidate formed by combining the Λ_c^+ candidate with a π^- or π^0 from the unassigned particle candidates of the event. This restriction is optimized using simulations and the optimal precision on the lifetime measurement is achieved by restricting the mass difference between the Ξ_c and Λ_c^+ candidates to two units of the mass resolution, removing events with $M(pK^-\pi^+\pi^-)$-$M(pK^-\pi^+)$ in [0.1834, 0.1864] GeV/c^2 or $M(pK^-\pi^+\pi^0)$ - $M(pK^-\pi^+)$ in [0.1753, 0.1873] GeV/c^2. About 61% of Ξ_c decays to Λ_c survive this veto, according to studies of simulated events. To account for the effect of the remaining background of this type, the measured Λ_c^+ lifetime is corrected by subtracting a bias of 0.34 fs, as discussed below.

After all selection criteria, the number of events in the Λ_c^+ signal range, defined as $M(pK^-\pi^+)$ in [2.283, 2.290] GeV/c^2, within about 1.4 units of the mass resolution around the world average Λ_c^+ mass, is 1.16×10^5. The relative amount of signal events, determined from a binned least-squares fit to the $M(pK^-\pi^+)$ distribution (Fig. 1), is 92.5%. In the fit, the $\Lambda_c^+ \to pK^-\pi^+$ signal is modeled as the sum of Gaussian and Johnson functions [29] with a common mode. The background is modeled as a linear function. Events from the Λ_c^+ sidebands, defined as $M(pK^-\pi^+)$ in [2.249, 2.264] GeV/c^2 and [2.309, 2.324] GeV/c^2, are used to constrain the background in the lifetime fit.

The Λ_c^+ lifetime is measured with an unbinned maximum-likelihood fit to the (t, σ_t) distribution for events in the signal region. The signal probability density function (PDF) is the product of an exponential function in t convolved with a Gaussian resolution function, which depends on σ_t, and a PDF for σ_t. The latter is a histogram template formed from signal candidates subtracted by the distribution of sideband candidates after scaling according to the size of the signal and background regions. To account for a possible bias in the decay-time determination, the mean of the resolution function is determined by the fit.

The background PDF, an empirical model of the sideband data, is the sum of two exponential functions convolved with Gaussian resolution functions, which account for backgrounds from long-lived particles, and a zero-
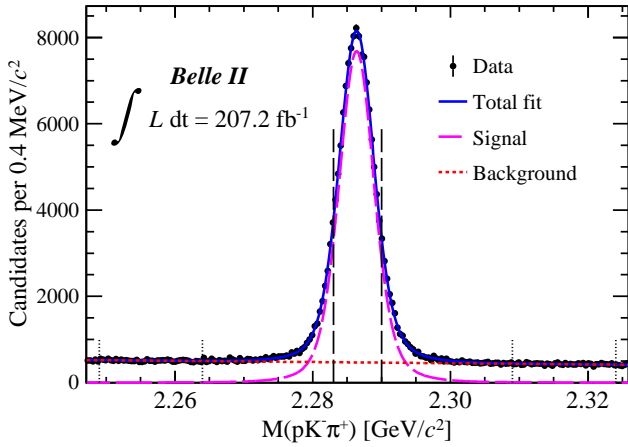
Figure 1: Mass distribution of $\Lambda_c^+ \to pK^-\pi^+$ candidates with fit projections overlaid. The vertical dashed lines enclose the signal region and the short, vertical dotted lines enclose the sidebands.
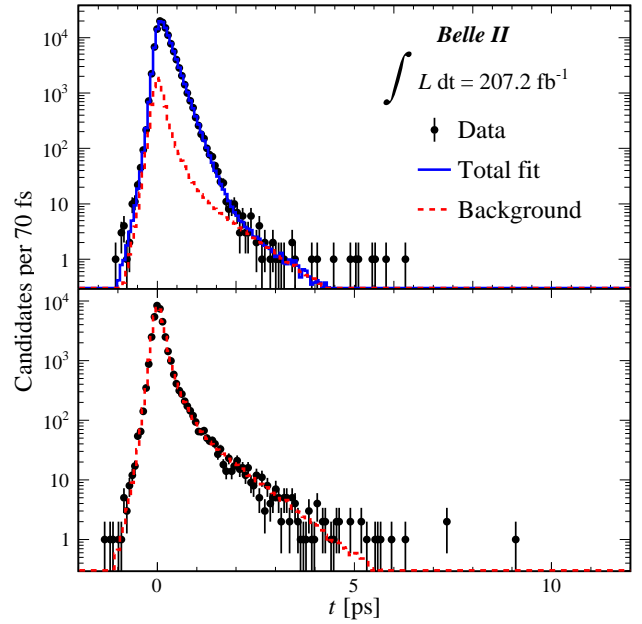

Figure 2: Decay-time distribution of $\Lambda_c^+ \to pK^-\pi^+$ events in the signal region (top) and sidebands (bottom) with fit projections overlaid.
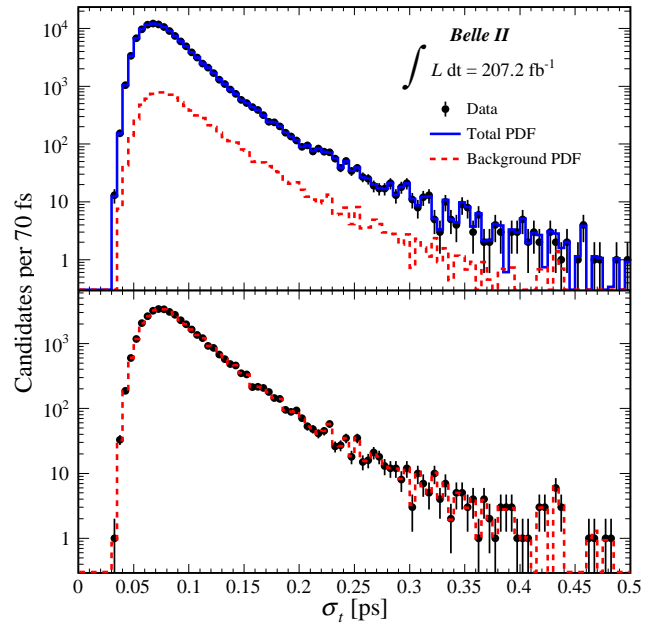

Figure 3: Decay-time uncertainty distribution of $\Lambda_c^+ \to pK^-\pi^+$ events in the signal region (top) and sidebands (bottom). The σ_t PDF used in the fit is shown by the solid blue histogram and the background σ_t PDF is shown by the dashed red histogram.

lifetime component consisting only of the resolution function, which accounts for combinatorial backgrounds. To account for a possible misestimation of the decay-time uncertainty, the width of the resolution function is given by the per-candidate σ_t multiplied by a scale factor, s, which is a free parameter in the lifetime fit. The mean of the resolution function is common for all terms, but a separate σ_t-scaling parameter is used for the background PDF.

To better constrain the background, a simultaneous fit to the events in the signal region and sidebands is performed, where the σ_t PDF for the sidebands is a binned template determined by sideband events. The background fraction in the lifetime fit is Gaussian constrained to $(7.50 \pm 0.02)\%$, as determined from the $M(pK^-\pi^+)$ fit.

The lifetime fit is validated both on fully simulated data equivalent to $1\,\mathrm{ab}^{-1}$, about five times the integrated luminosity of the collision data, and on simulated distributions generated by randomly sampling the lifetime PDF determined from a fit to the collision data. All validation fits return unbiased results, regardless of the assumed Λ_c^+ lifetime. Studies of the decay-time distribution in simulation suggest that σ_t is underestimated by about 10%, which is in good agreement with the results from the lifetime fit to the data, for which the scale parameter is determined to be s = 1.108 ± 0.006. The mean of the resolution function is determined to be 4.77 $\pm$ 0.63 fs.

The Λ_c^+ lifetime is measured to be $203.20 \pm 0.89\,\mathrm{fs}$, where the uncertainty is statistical only. The lifetime fit projection, overlaid on the decay time distribution in the data sample, is shown in Fig. 2. The σ_t PDF used in the lifetime fit is shown in Fig. 3. The systematic uncertainty is calculated from the sum in quadrature of

individual contributions from the sources listed in Table I and described below.

The systematic uncertainty due to backgrounds from Ξ_c decays is determined by adding simulated events of

Table I: Systematic uncertainties on the Λ_c^+ lifetime.

Source	Uncertainty [fs]
Ξ_c contamination	0.34
Resolution model	0.46
Non-Ξ_c backgrounds	0.20
Detector alignment	0.46
Momentum scale	0.09
Total	0.77

this type to the 1 ab^{-1} equivalent simulated sample according to the estimated maximum contamination determined from the fit to the distribution of the Λ_c^+ transverse vertex displacement in data and repeating the measurement. The difference between the simulated Λ_c^+ lifetime and the measured value is 0.68 fs. Since this is an estimate of the maximum effect of remaining Ξ_c backgrounds, half the difference, 0.34 fs, is taken as both a correction to the lifetime and an associated systematic uncertainty.

The resolution model for the lifetime PDF is complicated by correlations between the decay time and the decay-time uncertainty such that it cannot be described by a simple Gaussian function. We neglect these correlations in our model, which consists of a σ_t-dependent Gaussian resolution multiplied by a PDF in σ_t, and include the impact of this approximation as a systematic uncertainty. We fit our model to 1000 sets of signal-only simulated decays, each with a size equivalent to the data. The sets are produced by resampling, with repetition, simulated events in an amount corresponding to an equivalent luminosity of 1 ab^{-1}. The difference in the mean lifetime determined from these fits relative to the true value is 0.46 fs, which is taken as a systematic uncertainty due to the resolution model.

To check the resolution model, the lifetime fit is repeated with the Gaussian resolution function replaced with a sum of two Gaussian functions. The difference in the measured lifetime, 0.36 ± 0.23 fs, is covered by the corresponding systematic uncertainty. The bias of the decay-time resolution function for signal events depends on the Λ_c^+ candidate mass, but cancels if the signal range is centered on the true mass. Differences in the measured lifetime with the signal region varied are consistent with statistical fluctuations and are within the systematic uncertainty due to the resolution model.

Sideband events are included in the lifetime fit to constrain the background PDF. In simulation, sideband events describe the background distribution in the signal region accurately. To account for potential disagreements between the signal region and sidebands in the data, we produce 1000 sets of simulated data by resampling from the 1 ab^{-1}-equivalent simulated sample for events in the signal region and from the sidebands of the data sample for events in the sideband region. The mean lifetime

residual is 0.20 fs, which is taken as a systematic uncertainty associated with background contamination.

To check the signal PDF for the $M(pK^-\pi^+)$ fit, we replace the sum of Gaussian and Johnson functions with a sum of two Gaussian functions. Using the resulting background contribution has a negligible effect on the measured lifetime.

Reconstruction of charged particles at Belle II relies on periodic calibrations to correct for detector misalignment and surface deformations of the internal components of the PXD and SVD, as well as for relative alignments of the tracking system [30]. Detector misalignment can bias measured particle decay lengths and therefore their decay times. To account for imperfections in the detector alignment, sets of signal-only simulated data, each with a size comparable to the collision data, are produced with detectors randomly misaligned according to the alignment precision observed in data. The root mean square dispersion of the lifetime residuals in these misaligned simulated data sets is 0.46 fs, which is taken as a systematic uncertainty due to imperfect detector alignment.

The momenta of charged particles are scaled by a factor, 0.99971, determined by calibrating the peak positions of abundant charm, strange, and bottom hadron decays. The uncertainty on this scale factor, 0.0009, results in a systematic uncertainty on the Λ_c^+ lifetime of 0.09 fs. The uncertainty on the world average of the Λ_c^+ mass results in a negligible systematic uncertainty.

As a check of the internal consistency of the lifetime measurement, the full analysis is repeated on subsets of data chosen according to data-collection periods and Λ_c^+ momentum ranges, directions, and charge. The result for each subset is consistent with the full result. The lifetime fit is also repeated by selecting the candidate with the best vertex fit probability or randomly selecting a candidate, rather than rejecting events with multiple candidates. The difference in lifetime in each case is negligible. Finally, several events in the data have lifetimes greater than 4 ps, as shown in Fig. 2. Studies of simulated events suggest that these are from long lived charm meson decays and show that they do not bias the lifetime result with the current data-set size.

In conclusion, we measure the Λ_c^+ lifetime to be $203.20 \pm 0.89 \, (\text{stat}) \pm 0.77 \, (\text{syst})$ fs using data with an integrated luminosity of $207.2 \, \text{fb}^{-1}$ collected by the Belle II experiment at the SuperKEKB asymmetric-energy e^+e^- collider. This is consistent with the recent, relative measurement by LHCb [9] and other previous results, though the mild tension between the measurement by CLEO [14] and all other measurements remains. The absolute measurement presented here is the most precise Λ_c^+ lifetime measurement to date and may be useful to test the accuracy of HQE models as theoretical precision improves and discrepancies between theory and experiment become more significant.

This work, based on data collected using the Belle

[1] M. Neubert, Adv. Ser. Direct. High Energy Phys. **15**, 239 (1998), arXiv:hep-ph/9702375 .

[2] N. Uraltsev, in *At the frontier of Particle Physics*, edited by M. Shifman and B. Ioffe (2001) arXiv:hep-ph/0010328 .

[3] A. Lenz and T. Rauh, Phys. Rev. D **88**, 034004 (2013), arXiv:1305.3588 [hep-ph] .

[4] A. Lenz, Int. J. Mod. Phys. A **30**, 1543005 (2015), arXiv:1405.3601 [hep-ph] .

[5] M. Kirk, A. Lenz, and T. Rauh, JHEP **12**, 068 (2017), [Erratum: JHEP **06** (2020) 162], arXiv:1711.02100 [hep-ph] .

[6] H.-Y. Cheng, JHEP **11**, 014 (2018), arXiv:1807.00916 [hep-ph] .

[7] J. Gratrex, B. Melić, and I. Nišandžić, (2022), arXiv:2204.11935 [physics.hep-ph] .

[8] R. Aaij *et al.* (LHCb Collaboration), Phys. Rev. Lett. **121**, 092003 (2018), arXiv:1807.02024 [hep-ex] .

[9] R. Aaij *et al.* (LHCb Collaboration), Phys. Rev. D **100**, 032001 (2019), arXiv:1906.08350 [hep-ex] .

[10] R. Aaij *et al.* (LHCb Collaboration), Science Bulletin **67**, 479 (2022).

[11] P. A. Zyla *et al.* (Particle Data Group), PTEP **2020**, 083C01 (2020).

[12] J. M. Link *et al.* (FOCUS Collaboration), Phys. Rev. Lett. **88**, 161801 (2002), arXiv:hep-ex/0202001 .

[13] A. Kushnirenko *et al.* (SELEX Collaboration), Phys. Rev. Lett. **86**, 5243 (2001), arXiv:hep-ex/0010014 .

[14] A. H. Mahmood *et al.* (CLEO Collaboration), Phys. Rev. Lett. **86**, 2232 (2001), arXiv:hep-ex/0011049 .

[15] F. Abudinén *et al.* (Belle II Collaboration), Phys. Rev. Lett. **127**, 211801 (2021), arXiv:2108.03216 [hep-ex] .

[16] T. Abe *et al.* (Belle II Collaboration), (2010), arXiv:1011.0352 [physics.ins-det] .

[17] K. Akai, K. Furukawa, and H. Koiso, Nucl. Instrum. Meth. A **907**, 188 (2018), arXiv:1809.01958 [physics.acc-ph] .

[18] S. Jadach, B. F. L. Ward, and Z. Was, Comput. Phys. Commun. **130**, 260 (2000), arXiv:hep-ph/9912214 [hep-ph] .

[19] T. Sjöstrand *et al.*, Comput. Phys. Commun. **191**, 159 (2015), arXiv:1410.3012 [hep-ph] .

[20] D. J. Lange, *Proceedings, 7th International Conference on B physics at hadron machines (BEAUTY 2000): Maagan, Israel, September 13-18, 2000*, Nucl. Instrum. Meth. A **462**, 152 (2001).

[21] S. Agostinelli *et al.* (GEANT4 Collaboration), Nucl. Instrum. Meth. A **506**, 250 (2003).

[22] T. Kuhr, C. Pulvermacher, M. Ritter, T. Hauth, and N. Braun (Belle II framework software group), Comput. Softw. Big Sci. **3**, 1 (2019), arXiv:1809.04299 [physics.comp-ph] .

[23] V. Bertacchi *et al.* (Belle II tracking group), Comput. Phys. Commun. **259**, 107610 (2021), arXiv:2003.12466 [physics.ins-det] .

[24] S. Kurz, *Proceedings, Connecting the Dots 2020*, PROC-CTD2020-40, BELLE2-CONF-PROC-2020-009, NoStop

[25] J.-F. Krohn *et al.* (Belle II analysis software group), Nucl. Instrum. Meth. A **976**, 164269 (2020), arXiv:1901.11198 [hep-ex] .

[26] T. Lesiak *et al.* (Belle Collaboration), Phys. Lett. B **605**, 237 (2005).

[27] R. Aaij *et al.* (LHCb Collaboration), Phys. Rev. D **102**, 071101 (2020).

[28] P.-Y. Niu, Q. Wang, and Q. Zhao, Phys. Lett. B **826**, 136916 (2022).

[29] N. L. Johnson, Biometrika **36**, 149 (1949).

[30] T. Bilka *et al.*, EPJ Web Conf. **245**, 02023 (2020).